JOURNAL OF GEOPHYSICAL RESEARCH, VOL. 91, NO. C11, PAGES 12,887–12,897, NOVEMBER 15, 1986

Fine-Scale Variability at 140°W in the Equatorial Pacific

T. K. CHERESKIN, J. N. MOUM, P. J. STABENO, D. R. CALDWELL, AND C. A. PAULSON

College of Oceanography, Oregon State University, Corvallis

L. A. REGIER

Scripps Institution of Oceanography, La Jolla, California

D. HALPERN

School of Oceanography, University of Washington, Seattle

In November–December 1984 we carried out an intensive 12-day upper ocean sampling program on the equator at 140°W as part of the Tropic Heat Experiment. From our observations we constructed hourly averaged profiles of temperature, salinity, σ_t, turbulent kinetic energy dissipation rate, and horizontal velocity. These data were used to examine the correspondence between hydrographic and velocity fields and to compare the measured turbulent dissipations with the calculated Richardson numbers. We found that the core of the Equatorial Undercurrent tracked a density surface ($\sigma_t = 25.25$) on times as short as 1 hour. The variability in both hydrographic and velocity fields was greatest at the semidiurnal frequency. The supertidal energy was not significantly different from the Garrett-Munk mid-latitude level once latitudinal scaling was removed from the Garrett-Munk model parameters. Horizontal velocity spectra were found to be contaminated by displacement of the background shear. Turbulent dissipation was dominated by a dirunal cycle, with high values of dissipation occurring at night above the undercurrent core. Shear and buoyancy frequency, calculated over 12-m vertical scales, were observed to track each other above the core and were dominated by a diurnal period above 40 m and by a semidiurnal period below 40 m. When shear and buoyancy frequency were combined to form a Richardson number, neither diurnal nor semidiurnal cycles were present. Above the undercurrent core, the Richardson numbers were uniformly small (0.3 to 0.6).

1. INTRODUCTION

Studies have suggested that space and time variability in the equatorial ocean may be quite different from variability at mid-latitudes. Internal wave spectra from the equatorial Indian Ocean indicate more energy at frequencies above the tidal than is predicted by the Garrett-Munk (GM) universal internal wave spectrum [*Eriksen*, 1980]. Other deviations from GM [*Garrett and Munk*, 1972, 1975] include less spatial coherence [*Wunsch and Webb*, 1979; *Eriksen*, 1980] and an excess of horizontal kinetic energy over potential energy at subtidal frequencies [*Eriksen*, 1980]. One obvious difference is that at the equator there is no Coriolis parameter to limit the frequency bandwidth of internal waves.

From their fine-structure measurements, *Toole and Hayes* [1984] found enhanced shear and strain variance and a greater proportion of low values of the Richardson number on the equator. *McPhaden* [1985] noted anomalously high fine-scale temperature and density variance confined within 1° of the equator. Microstructure measurements indicated a peak in turbulent kinetic energy dissipation rate within 1° of the equator [*Crawford*, 1982], but more recent results [*Moum et al.*, 1986*b*] have shown this peak to be an artifact of the sampling limitations of the previous study.

In November–December 1984 we carried out an intensive 12-day sampling program near the equator at 140°W as part of the Tropic Heat experiment. Vertical profiles of temperature, conductivity, and small-scale shears were obtained every 10 min (on average) with the rapid sampling vertical profiler (RSVP). Vertical profiles of horizontal currents were obtained every 30 s with a shipboard acoustic Doppler current profiler (ADCP). From these data we constructed hourly averaged profiles of temperature T, salinity S, σ_t, kinetic energy dissipation rate ε, and horizontal velocity. Using these series of profiles we made the following observations and comparisons:

1. We examined the correspondence between hydrographic and velocity fields. We found that the core of the Equatorial Undercurrent (EUC) tracked a density surface ($\sigma_t = 25.25$) on times as short as 1 hour. The core tracked the salinity maximum almost as well.

2. We compared the high-frequency variability with that observed at other latitudes in terms of the Garrett-Munk model. We found that (1) the time variability in both hydrographic and velocity fields was greatest at the semidiurnal frequency, (2) the supertidal energy was not significantly different from the Garrett-Munk mid-latitude level once the latitudinal scaling was removed from the Garrett-Munk model parameters, and (3) the horizontal velocity spectra were contaminated by displacement of the background shear.

3. We compared calculated Richardson numbers with the observed values of turbulent kinetic energy dissipation rate and found that (1) the dissipation was dominated by a diurnal cycle, with high values occurring at night above the undercurrent core, (2) shear and buoyancy frequency calculated over 12-m scales tracked each other extremely well, with a diurnal cycle above 40 m and a semidiurnal cycle below 40 m and (3) the Richardson number was uniformly small (between 0.3 and 0.6) above the undercurrent core. For the 12-day period, the Richardson number displayed neither a diurnal nor a semidiurnal periodicity. (In longer times series, periods were observed when the Richardson number cycled diurnally near the surface.)

Paper number 6C0326.
0148-0227/86/006C-0326$05.00

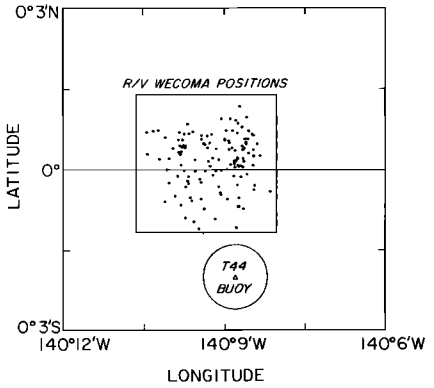

Fig. 1. R/V *Wecoma* positions (diamonds) determined from satellite fixes during the 12-day station. The location of the T44 buoy (triangle) is also shown. The *Wecoma* measurements were made within a box that was 4.8 km square. The distance between the buoy and the mean *Wecoma* position was 4 km. The uncertainty in the buoy position is 1 km.

2. MEASUREMENTS

The measurements consisted of wind, humidity, solar and infrared radiation, horizontal currents, air and water temperature, electrical conductivity, and small-scale shears. They were made on the equator near the Equatorial Pacific Ocean Climate Study/Tropic Heat T44 buoy (located at 0°2'S, 140°9'W) from November 19 to December 1, 1984. In order to maintain position near the buoy in the westward surface current, the ship was repositioned whenever it drifted outside of a 4.8 × 4.8 km box centered 4 km north and slightly west of the T44 mooring (Figure 1).

Horizontal velocity estimates were obtained with an acoustic Doppler current profiler; the instrument has been described by *Regier* [1982]. The profiler transmits 300 kHz in 20.4-ms pulses along four beams that point 60° downward from the horizontal. Sound is reflected back to the transducers by scatterers assumed to be passive tracers of the water motion. The measured frequency shift between transmitted and reflected pulses determines the water velocity relative to the ship. Range gating the return (using 6.2-ms bins) produces a vertical profile of velocity at 4-m intervals down to 260 m. Strong echo returns give reliable velocity estimates down to 200 m. Because of the finite pulse length and the range gating, the velocities are effectively filtered by a trapezoidal filter that is the convolution to two unit gates of widths 6.2 and 20.4 ms. Totally independent estimates of velocity are obtained every 17.7 m. Since the filter is tapered, the estimates are nearly independent every 12 m. Ten-minute averaging resolves relative velocity within 1 cm s^{-1}. The velocities described here were averaged in time over 1 hour. Obtaining absolute velocities from the relative velocities requires either precise navigation or an independent estimate of the current at some depth to remove the motion of the ship. For our 12-day station the ship motion was removed from the ADCP profiles by referencing the hourly averages to the hourly averaged current meter observations at 25-m depth on the T44 mooring. Root-mean-square differences of hourly averages at the other four depths where current meter measurements were available ranged from 5 to 10 cm s^{-1} (Table 1); a detailed comparison has been made by T. K. Chereskin et al. (manuscript in preparation, 1986).

Fine-scale hydrography measurements were obtained from a microstructure profiling instrument, the rapid sampling vertical profiler. The RSVP has sensors which measure pressure, temperature, electrical conductivity, and small-scale shears; the instrument has been described by *Caldwell et al.* [1985]. It descends through the water on a cable which is kept slack to isolate the sensors from ship motion. The cable carries power to the instrument and returns signal to the ship for recording. Temperature was measured with a Thermometrics FP14 thermistor, conductivity was measured with either a Neil Brown Instrument Systems sensor or a four-electrode microconductivity probe, and shears were measured using Undersea Technology airfoil probes. The depth resolution of each measurement is approximately several centimeters. For the purposes of the study presented here, the values of temperature, salinity, and σ_t were averaged vertically over 1 m. Estimates of turbulent kinetic energy dissipation were made from the small-scale shears (spatial scales of 1.5 to 50 cm).

3. HORIZONTAL CURRENTS AND FINE-SCALE HYDROGRAPHY

This description will focus on the east-west component of velocity and the Equatorial Undercurrent. It should be noted that these measurements were made during the northward phase of a 20-day oscillation in the north-south component of velocity. An oscillation at a period of 16–30 days has been observed in both the tropical Atlantic and the tropical Pacific [*Duing and Hallock*, 1980; *Legeckis*, 1977]; it is thought to result from an instability of the mean current [*Philander*, 1978]. Two years of data at the T44 mooring site revealed the seasonal cycle in the currents, with November 1984 appearing quite similar to November 1983 but decidedly different from April 1984. The time series from the T44 mooring indicated southward flow from November 10 to 20, the flow turned northward by November 21 and remained northward until December 1. Prior to our arrival on station we completed a transect of currents and fine-scale hydrography from 3°N to 3°S along 140°W from November 15 to 18 [*Moum et al.*, 1986*b*]. These measurements also indicated southward flow from 3°N to 2°S, where we crossed a sharp surface front and observed northward flow to the south of the front. The transect also defined the width of the EUC high-velocity core (about 1°) and showed an undercurrent centered just north of the equator.

Plate 1*a* shows the contours of north-south velocity derived from the ADCP measurements, referenced as was described in section 2 using hourly current meter observations. (Plate 1 is shown here in black and white. The color version can be found in the separate color section in this issue.) During the first 4 days of the station the flow was weakly northward, followed by large northward flow (greater than 50 cm s^{-1}) above 100 m for the remainder of the station. The northward velocity occurred at depths shallower than the depth of the

TABLE 1. Root-Mean-Square Differences Between Hourly Averaged ADCP Currents and VACM Currents Measured at Four Depths on Mooring

Depth, m	rms *u*, cm s^{-1}	rms *v*, cm s^{-1}
45	6.3	5.3
80	6.8	5.8
120	6.6	8.6
160	10.8	8.5

ADCP currents are referenced using VACM at 25-m depth on T44 mooring.

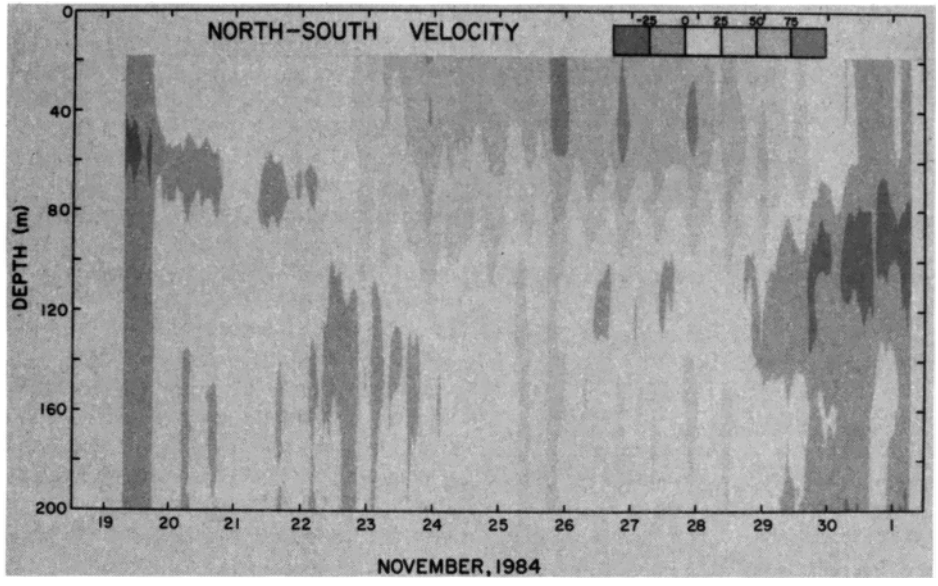

Plate 1*a*

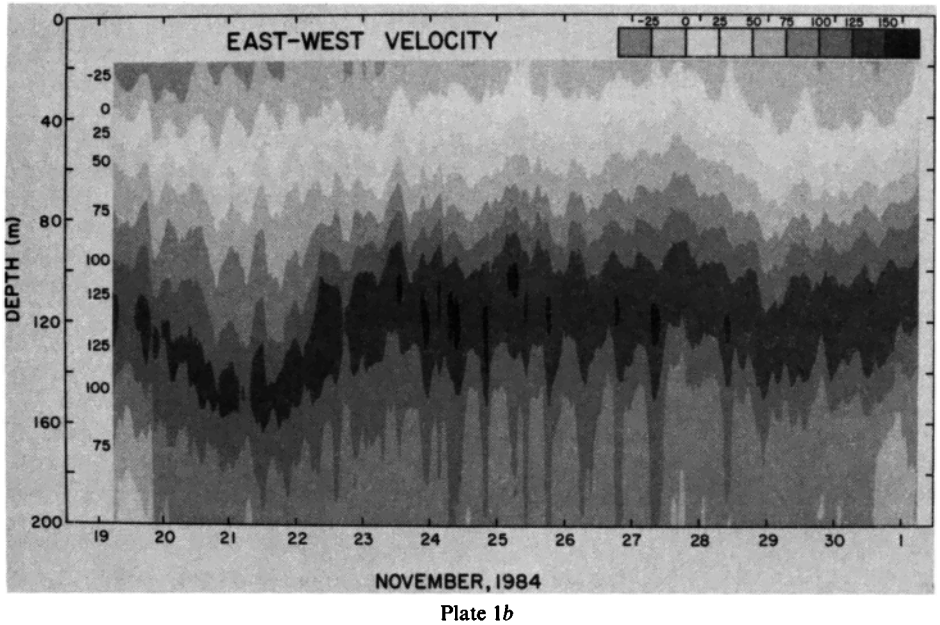

Plate 1*b*

Plate 1. Hourly averages of (*a*) north-south current and (*b*) east-west current, in centimeters per second, from the shipboard ADCP referenced using hourly currents at 25 m from the T44 buoy. (The color version of this figure can be found in the separate color section in this issue.)

EUC (120 m). The shear of the north-south current is also evident in Plate 1*a*. At all depths the east-west shear was at least twice the north-south shear.

The contours of east-west velocity are shown in Plate 1*b*. The maximum eastward speeds observed were in excess of 150 cm s^{-1}, with the core located at approximately 120-m depth. There were two dominant time scales: the semidiurnal tide and the 4-day pulse. During the first 4 days of the measurement period, a large-amplitude pulse was observed in velocity. Associated with this pulse were a downward displacement of the velocity maximum (about 30 m) and a decrease in velocities in the core (no speeds as great as 150 cm s^{-1}); above the core we observed lower values of shear, higher Richardson numbers and lower values of kinetic energy dissipation than we observed during the remaining 8 days. The thermocline and salinity maximum were also displaced downward approximately 30 m.

The internal tide dominated the fluctuations of both velocity components, with associated peak-to-peak vertical displacements of the order of 10 m. The semidiurnal peak appears especially prominent owing to a change in slope at the tides (Figure 2). At frequencies above the tidal, a $(\text{frequency})^{-2}$ slope is a reasonable fit to the spectral shape. However, the spectral shape at lower frequencies then appears either as a deficit in energy or as a change in slope. In either case, the semidiurnal frequency is distinctive. *Eriksen* [1980] observed a similar disparity in slope above and below the tides in Indian Ocean equatorial waves. The vanishing of the Coriolis parameter f at the equator removes the lower cutoff frequency for internal gravity waves, which at mid-latitudes normally occurs just below the tides.

Plates 2*a*, 2*b*, and 2*c* show the contours of temperature, salinity, and σ_t respectively, obtained from the RSVP. (Plate 2 is shown here in black and white. The color version can be

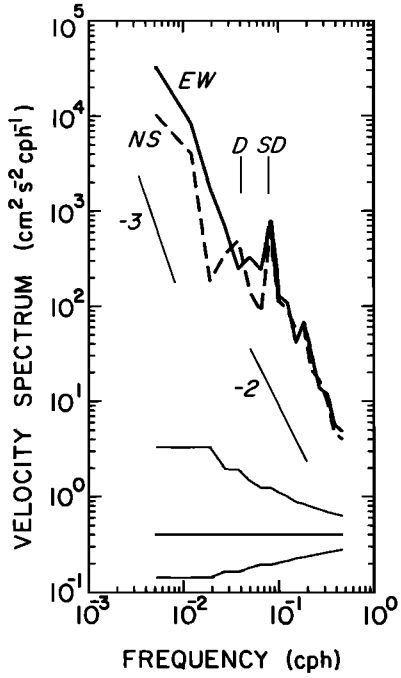

Fig. 2. Autospectra of east and north velocity from the T44 current meter at 120 m. Note the peak at semidiurnal frequency (SD) and the change in slope across the tides. The dashed curve is north. Diurnal frequency is indicated by D.

found in the separate color section in this issue.) The data have been depth averaged to 1 m and time averaged over hourly intervals prior to contouring. The same two time periods evident in the east-west velocity section (Plate 1*b*) are plainly evident in the hydrographic sections: a large-amplitude displacement or pulse of 4-day duration occurring at the start of the measurement period and the semidiurnal oscillation. The pulse, in addition to depressing the EUC, also weakens the gradients above the core. Displacement spectra of six isopycnal surfaces clearly show the dominant semidiurnal peak and the change in slope at subtidal frequencies (Figure 3*a*).

We found the core of the EUC to lie in the thermocline, in the temperature range from 18° to 21°C. It tracked the salinity maximum, salinity greater than 35.40 parts per thousand (ppt), extremely well. However, the core followed even more closely the density surface, $\sigma_t = 25.25$ (Figure 4). The highest correlation was between the velocity maximum and σ_t (correlation of 0.94); the velocity maximum appeared to fall at or just below the salinity maximum. *McPhaden* [1985] also found the core to lie at or below the salinity maximum and found significant intrusive variability over this depth range.

We believe the high salinity observed in the core to be the salinity front associated with the equatorial current system [*Wyrtki and Kilonsky*, 1982]. A lens of high-salinity water at 120- to 130-m depth extending from the equator to 3°S was observed in the N-S transect made prior to the equatorial station [*Park et al.*, 1985]. At the time of the transect the maximum thickness of the high-salinity lens was located at approximately 0.25°S, the EUC was centered at 0.25°N, and the surface South Equatorial Current was centered at 0.75°N [*Moum et al.*, 1986*b*].

Near-surface changes in temperature and salinity were also observed and may be due to the advection of a surface front by the 20-day oscillation. The time series of temperature and salinity showed substantial change in the upper 40–60 m over the 12-day time period. Salinity increased by 0.3 ppt, and temperature warmed by 1°–2°C. During the N-S transect we observed a distinct front at 1.5°S, with relatively cold, fresh water to the north (<24°C, <35.0 ppt) and warm, salty water to the south (>24°C, >35.1 ppt). Southward velocities were observed to about 2°S; this time period corresponded to the southward phase of the 20-day oscillation observed in the moored current meter data on the equator. If the 20-day oscillation extended as far south as 1.5°S, then the changes that we observed during our station may be attributed to the advection of the front observed at 1.5°S. During our first 4 days on station the northward current was weak; the weak flow was followed by flow at about 50 cm s^{-1} (50 km day^{-1}) for the remainder of the station. If the current was of this magnitude as far south as 1.5°S, then one might expect to see the front advect past approximately 3 days after the onset of large northward flow (on November 26). It is suggestive that the σ_t section indicates an abrupt change at this time. However, advection of the front from 1.5°S is speculation; we do not have current measurements off the equator during this time period. Only south of the front did we find water with the correct *T-S* properties to account for the observed changes. Another possibility is that the change may be due to advection from the east by the surface current.

The diurnal cycle of the surface mixed layer is apparent in the 24°C isotherm (Plate 2*a*) and the 23.50 isopycnal (Plate 2*c*) during the first 3 days of the time series. Time axis ticks occur at 1200 UT, corresponding to 0200 LT. The isotherm depth excursion is of the order of 20 m. On later days the diurnal cycle is present but is not revealed by the chosen contour intervals.

4. Spectral Shapes and Levels

The Garrett-Munk universal wave spectrum is a description of the internal wave field based on observations and linear wave theory. As a spectral description it has proved remarkably robust in representing the internal wave field, even when linear theory breaks down. The GM spectrum may represent an equilibrium state for the internal wave field. A test of this has been to use the GM description as a framework within which to compare measured internal wave spectra from different parts of the world ocean. The GM model assumes a linear superposition of internal waves with random phases, horizontal isotropy and vertical symmetry, and the WKBJ approximation for wave functions in both the vertical and latitudinal variables. The last assumption restricts the model to wave frequencies ω where $f \ll \omega \ll N(z)$. It also restricts the model to latitudes away from the equator, where f is a rapidly varying function of latitude.

Eriksen [1980] has attempted to extend the GM model to describe spectra from the equatorial Indian Ocean. He argues that at high frequencies the scales of the waves are small enough that they are not influenced by the earth's rotation and should merge smoothly with the GM f plane model. At lower frequencies he constructed a model description in the spirit of GM which takes into account equatorial wave modes: Kelvin, mixed Rossby-gravity, and inertial internal waves. These modes were not resolved by our short time series. Most of Eriksen's observations were deep (below 1000 m); it is these observations that he attempted to model. Our observations were all in the upper 200 m.

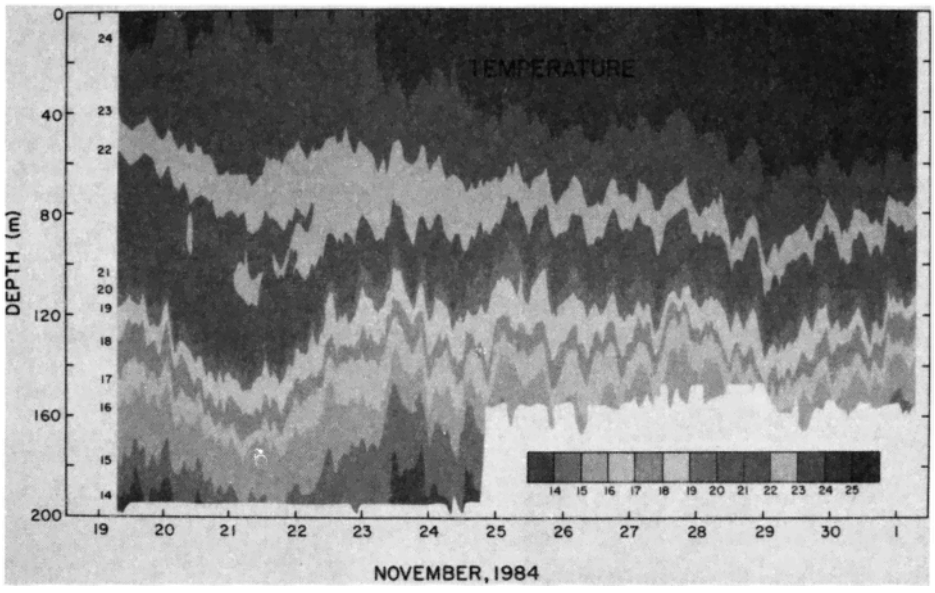

Plate 2*a*

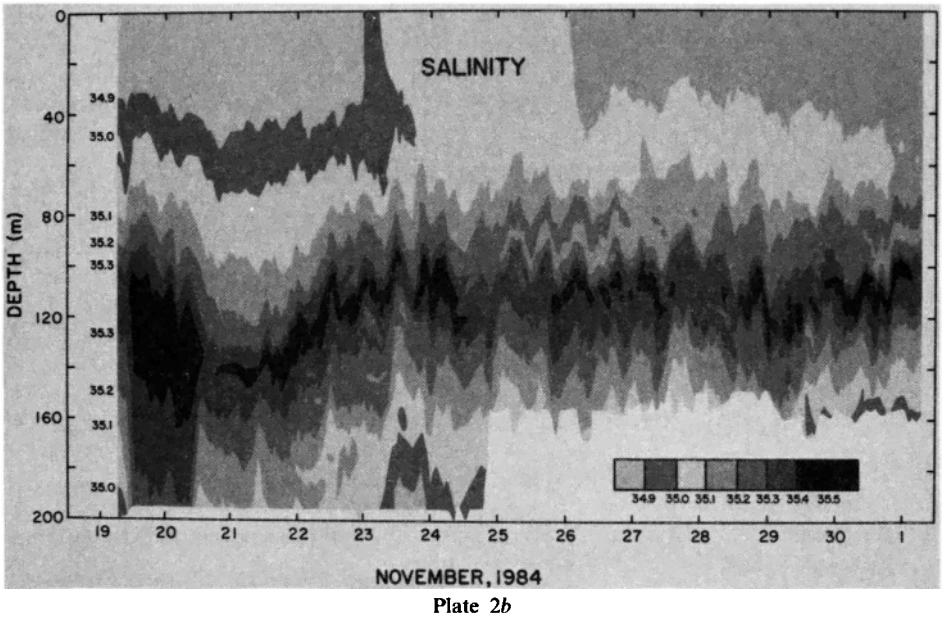

Plate 2*b*

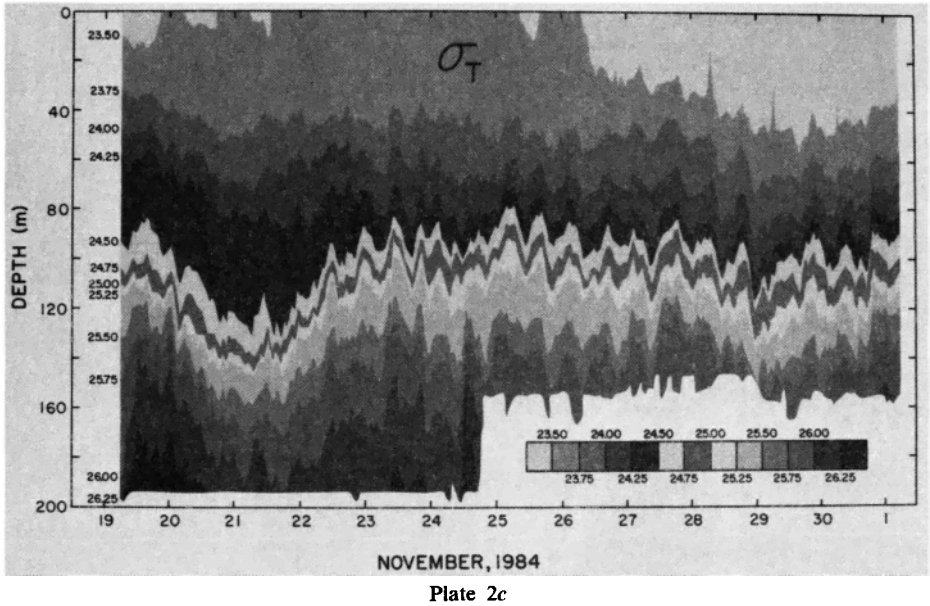

Plate 2*c*

Plate 2. (*a*) Isotherm depths calculated from hourly averages of temperature in degrees Celsius. (*b*) Isohaline depths calculated from hourly averages of salinity in parts per thousand. (*c*) Isopycnal depths calculated from hourly averages of σ_t. (The color version of this figure can be found in the separate color section in this issue.)

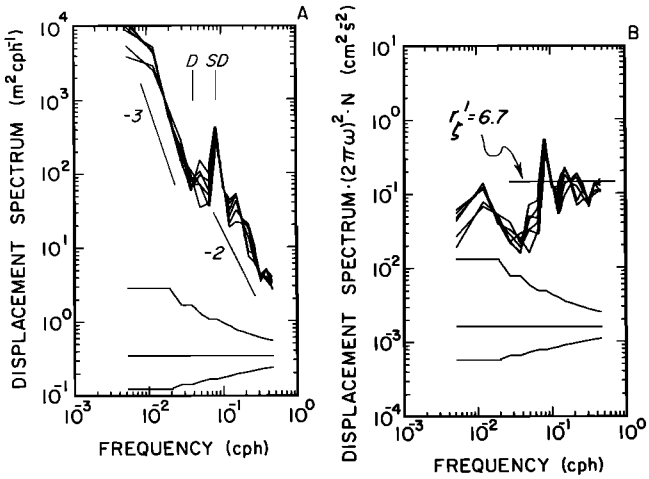

Fig. 3. (*a*) Autospectra of isopycnal displacement from six σ_t surfaces (24.00–25.25). At low frequencies the two less energetic spectra correspond to isopycnals which lie above the large-amplitude 4-day pulse. The other four spectra correspond to isopycnals which lie within the large-displacement region. Note the large peak at the semidiurnal tide (SD) and the discontinuity in slope across the tide. Diurnal frequency is also indicated (D). (*b*) Vertical velocity spectra calculated from the displacement spectra of Figure 3*a* by multiplying by frequency squared and applying WKBJ N scaling (N = 6 cph). Also shown is the GM level corresponding to r' ($=r_\zeta'$) = 6.7.

Although the spectral shape which *Eriksen* [1980] observed for the high frequencies was consistent with GM (ω^{-2}), one can ask whether or not the spectral level is also consistent. Estimating the GM level parameter from an observed spectrum yields very high levels for near-equatorial spectra compared with canonical GM values. This is a consequence of the latitudinal scaling of the model; *Munk* [1981] has suggested that this scaling be removed. *Levine et al.* [1985] have proposed a new level parameter that removes the GM f scaling. They compared level parameters estimated from spectra from a wide range of latitudes (including Eriksen's Indian Ocean spectra) and found that equatorial levels were comparable to mid-latitude levels when f scaling was removed.

We follow their approach in estimating the level parameters for our displacement and velocity time series. The GM model is characterized by four parameters: b (buoyancy depth scale, in meters), N_0 (buoyancy frequency scale, in cycles per hour), j_* (nondimensional mode number), and E (nondimensional energy level). *Desaubies* [1976] has shown that the model can be characterized by just two independent parameters

$$r = Eb^2N_0$$

$$t = j_*/(2N_0b)$$

The frequency spectra of vertical displacement and horizontal velocity are written

$$S_\zeta(\omega) = (2rf)(\pi N)^{-1}(\omega^2 + f^2)^{1/2}\omega^{-3} \quad (1)$$

$$S_u(\omega) = S_v(\omega) = (4\pi rfN)(\omega^2 + f^2)(\omega^2 - f^2)^{-1/2}\omega^{-3} \quad (2)$$

where frequency ω, Coriolis parameter f and buoyancy frequency N are in cycles per hour. S_ζ has units of m² cph⁻¹, and S_u has units of m² h⁻² cph⁻¹. *Levine et al.* [1985] removed f scaling from the determination of the level r by defining a new level parameter r'

$$r' = rf \quad (3)$$

with units of m² cph². By determining r' instead of r, singularities caused by the factor $1/f$ are removed. We calculated two estimates of r': r_ζ' from vertical dispacement and r_u' from horizontal velocity.

In the spectra of displacement calculated for six different σ_t surfaces, the semidiurnal peak dominates, with a change in slope at the internal tide (Figure 3*a*). The tidal harmonics are also evident, and the high-frequency slope is −2. Vertical velocity spectra were calculated from displacement by multiplying by frequency squared and applying WKBJ N-scaling (Figure 3*b*). The level r_ζ' estimated from the vertical velocity specrum and (1) is 6.7 ± 5 m² cph². This level falls within the main grouping of values shown by *Levine et al.* [1985] (see their Figure 7*b*); it is lower than most other equatorial measurements.

Figure 2 shows the velocity spectra from the T44 current meter at 120-m depth. Using (2) and the spectral energy densities at frequencies much higher than that of the tide, we estimated a level r_u' = 28.8 ± 10 m² cph². This level is similar to other equatorial measurements, but is a factor of 4 larger than r_ζ', our estimate of r' calculated from displacement spec-

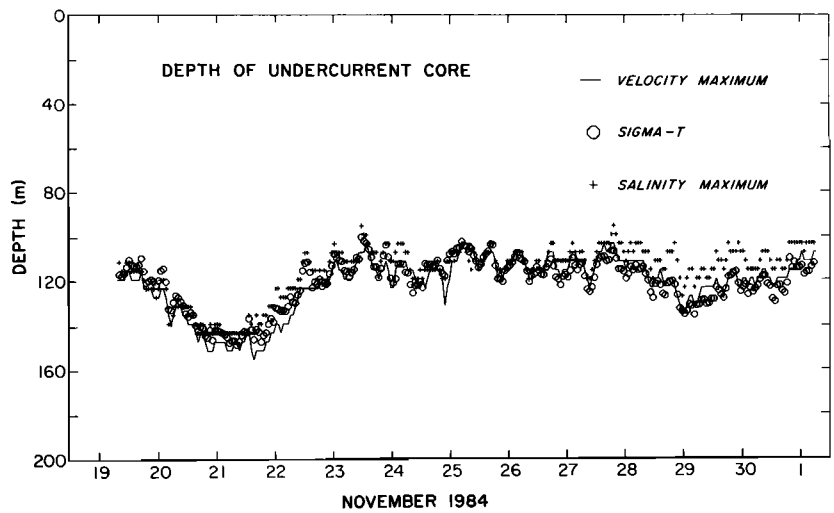

Fig. 4. Depth of three surfaces: velocity maximum (solid line), σ_t = 25.25 (open octagons), and salinity maximum (crosses).

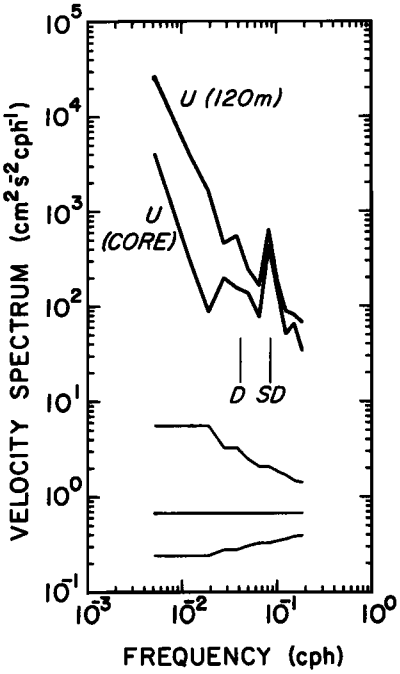

Fig. 5. Autospectra of east velocity measured by the shipboard ADCP: the more energetic spectrum is the velocity at fixed depth (120 m); the less energetic is the spectrum of velocity at the depth of the velocity maximum (along the density surface $\sigma_t = 25.25$). At low frequencies the spectrum at fixed depth is pumped up by large-amplitude displacement in a background shear. At the semidiurnal frequency (SD), typical displacements are of the order of the accuracy with which we can track the core, and the two spectra merge. The spectra have been arbitrarily truncated at high frequency, since the core is not accurately tracked on the smallest resolvable time scales. Diurnal frequency is indicated by D.

tra. The difference between these two independent estimates of spectral level can be reconciled by considering the large shear of the EUC and the vertical velocity field.

To understand the effect of shear and a fluctuating vertical velocity on the horizontal velocity measured at a fixed depth, we consider an idealized, undisturbed velocity profile

$$U(z) = A + Bz \tag{4}$$

We can think of $U(z)$ as the steady state EUC in the absence of internal wave motion. The shear U_z is linear, $U_z = B$.

If we now superimpose wavelike perturbations u' and ζ on this background flow, we can express the horizontal velocity u^* measured at a depth z as

$$\begin{aligned} u^*(z, t) &= U(z - \zeta) + u'(z, t) \\ &= A + Bz - B\zeta + u' \end{aligned} \tag{5}$$

Equation (5) states that the time-varying velocity u^* that we measure at depth z can be attributed to local horizontal velocity fluctuations u' at depth z and to the vertical oscillation of the background flow field $U(z - \zeta)$, where ζ is the time-varying displacement.

If we time average (denoted by angle brackets) equation (5), we find that (assuming linear oscillations $\langle u' \rangle = \langle \zeta \rangle = 0$)

$$\langle u^* \rangle = A + Bz \tag{6}$$

Because the background shear is linear, the mean flow is just the backgroud state, i.e., $\langle u^* \rangle = U$. If we had included a quadratic term in our model of $U(z)$, the mean flow would differ from the undisturbed flow. To look at velocity fluctuations about the mean, we subtract $\langle u^* \rangle$ from both sides of (5) and define u as follows:

$$u = u^* - \langle u^* \rangle = -B\zeta + u' \tag{7}$$

Fourier transforming and taking the spectrum yields

$$S_u = S_\zeta B^2 + S_{u'} \tag{8}$$

We have neglected the term involving the cross spectrum of ζ and u'. For the GM model this term would vanish identically. Although it may not be zero here, it is no larger than the two remaining terms whose relative magnitude we now estimate. The velocity spectrum that we measure is S_u. The velocity spectrum that the GM model ($B = 0$) predicts is $S_{u'}$. We can estimate how much shear is required to account for the difference between S_u and $S_{u'}$ using (8). We estimate S_u using (2) and

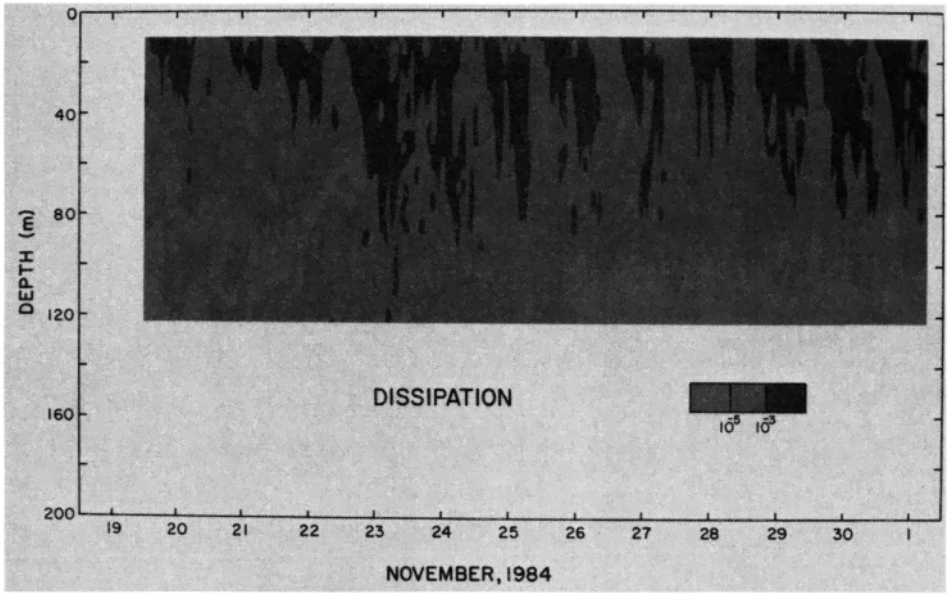

Plate 3. Dissipation (in $cm^2\ s^{-3}$) contoured at 2-decade intervals, depth averaged over 5 m, and time averaged over 1 hour. High dissipations occur at night, with the deepest dissipations extending to 90 m. (The color version of this figure can be found in the separate color section in this issue.)

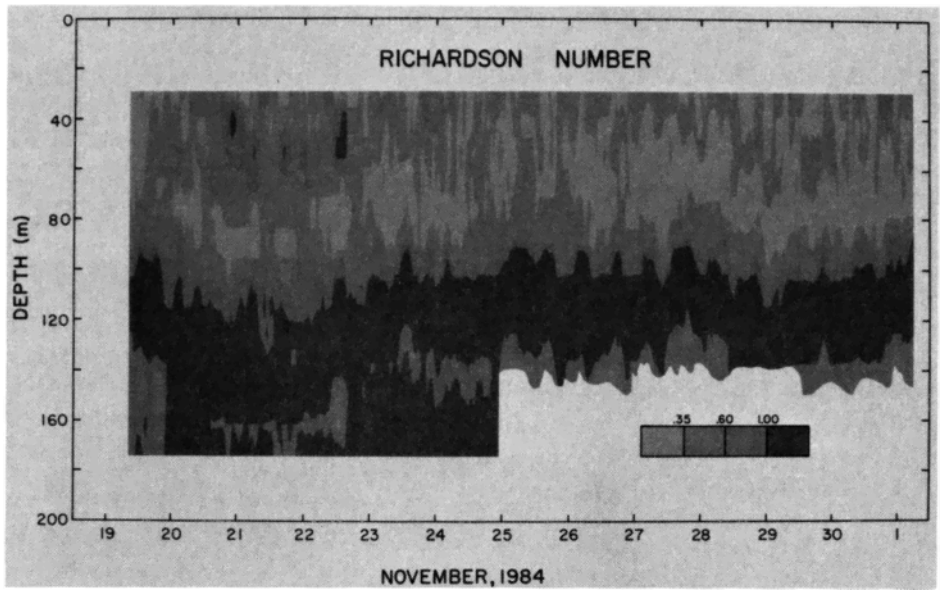

Plate 4. Contours of hourly averaged Richardson number calculated over 12-m vertical scales (0.35, 0.60, and 1.00). Above the core the Richardson number was low (below 0.60). The core was distinguished as a region of high Richardson number (above 1.0). High values of Richardson number occurred above 75 m during the first 4 days, corresponding to lower shear associated with the pulse. (The color version of this figure can be found in the separate color section in this issue.)

values of $\omega = 0.3$ cph, and $r_u' = 29$. We use (1) and (2) with a value of $r_\zeta' = 7$ to estimate S_ζ and $S_{u'}$. The shear required is 0.013 s^{-1}. The measured shear associated with the EUC ranges from 0.005 s^{-1} in the shear minimum region to greater than 0.025 s^{-1} above the core. The shear required to balance (8) is well within the range of that observed and indicates that the horizontal velocity spectra are strongly contaminated by the displacement of the background shear flow. In fact, if no u' were present, a horizontal velocity would still be measured from the vertical displacement of the mean flow. If $S_{u'}$ were zero, a shear of 0.015 s^{-1} would be required to balance the two remaining terms in (8)! An upper bound shear estimate calculated for an upper bound estimate of $r_u' = 39$, a lower bound estimate of $r_\zeta' = 2$, and $S_{u'} = 0$ yields 0.032 s^{-1}.

The simple model which we have presented applies at all frequencies, not just for supertidal ones. We also found evidence that the levels of the velocity spectra at tidal frequencies and below were being pumped up by vertical advection of the background shear. Figure 5 compares the u velocity following the density surface at the core and the velocity at the mean (fixed) core depth, 120 m. Both estimates are from ADCP measurements. At low frequency, when the large-amplitude pulse displaces the core by 30 m, the spectrum at a fixed depth shows a much higher level (factor of 7) than the spectrum following the core. The displacements at tidal frequency are of order of 10 m, the accuracy with which we can track the depth of the core. Thus at frequencies at and above the semidiurnal we can no longer resolve the effect of the displacement of the background shear by tracking the core. However, at these supertidal frequencies the different estimates of GM level parameters have shown the influence of shear flow.

5. Dissipation, Shear, N, and Richardson Number

Hourly values of turbulent kinetic energy dissipation rate ε depth-averaged over 5 m and contoured at 2 decade intervals showed a distinct diurnal cycle (Plate 3). (Plate 3 is shown here in black and white. The color version can be found in the separate color section in this issue.) The diurnal mixing cycle during Tropic Heat has been documented by *Moum and Caldwell* [1985] and *Gregg et al.*, [1985]. High values occurred at night, with the largest values generally confined to the top 40–60 m. Lower nighttime values of dissipation were associated with the 4-day pulse, and low values occurred throughout the shear minimum region of the core (120 m). On November 23, high values of dissipation extend as deep as 90 m. Typically, high values at depth were observed approximately 1–2 hours after the high values near the surface. The diurnal cycling suggested that nighttime convective mixing played an important role in the dissipation cycle.

Hourly averaged Richardson number estimates were calculated on 12-m vertical scales using the density estimates from the RSVP and the ADCP shears. The Richardson number, $N^2/(U_z)^2$, is often interpreted as an index to turbulent mixing caused by Kelvin-Helmholtz instability of a stratified shear flow. Instability occurs when the Richardson number falls

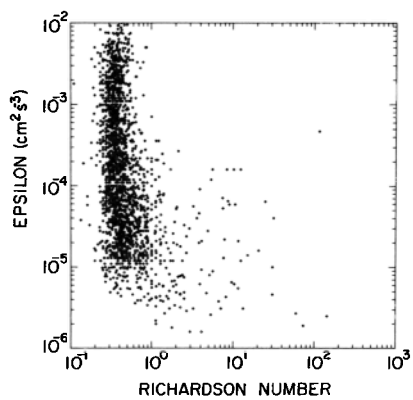

Fig. 6. Dissipation versus Richardson number, hourly averages over 12-m vertical scales. High dissipations occurred only for low Richardson numbers, and high Richardson numbers occurred only for low dissipations.

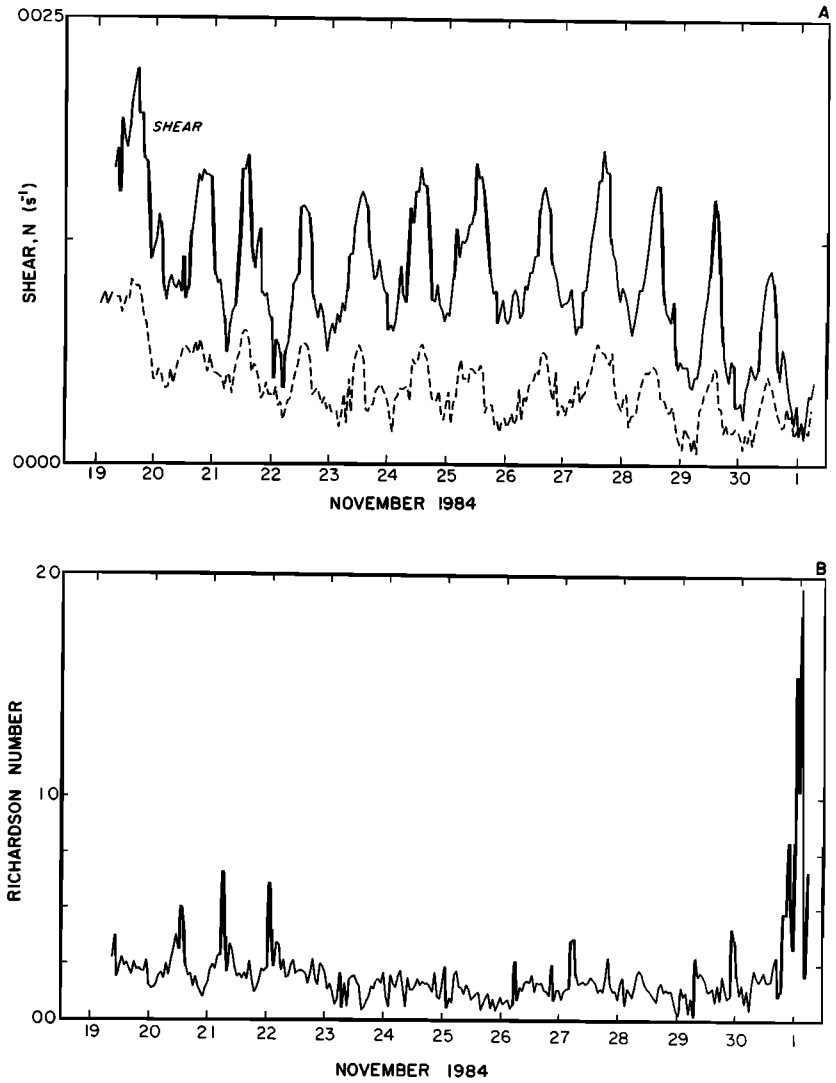

Fig. 7. (*a*) Time series of hourly averaged shear and N at 17.5 m. Shear was calculated from current meters at 10 and 25 m. N was computed from RSVP measurements. Shear and N cycle diurnally, with the same relative magnitude and in phase. (*b*) Time series of Richardson number at 17.5 m calculated from shear and N. There was no diurnal cycle in the Richardson number.

below 0.25 [*Miles and Howard*, 1964]. Contours of Richardson number (Plate 4) indicated that above the core the Richardson numbers typically fell below 0.60, with patches of higher values. (Plate 4 is shown here in black and white. The color version can be found in the separate color section in this issue). About 75% of the values above 90 m fell between 0.2 and 0.5. The core was distinctive as a region of high Richardson number (larger than 1). Higher Richardson numbers also occurred above 75 m during the first 4 days, corresponding to lower shears associated with the pulse. A direct comparison (Figure 6) of dissipation and Richardson number (using dissipations calculated on 12-m vertical scales) indicated that when the dissipation was high the Richardson number was less than 1 and when the Richardson number was high the dissipation was low. However, for low Richardson numbers a large range of dissipations were observed.

The Richardson number contour section indicated that the high-shear region above the EUC core was only marginally stable (see also *Moum et al.* [1986*a*]). Although ε exhibited a strong diurnal signal, the Richardson number did not. It may be that averaging both vertically and in time lowered the correlation between these two quantities. It is surprising to see how well stratified shear flow dynamics work to maintain marginally supercritical Richardson numbers.

Although Richardson numbers were not observed to cycle diurnally, both the shear and the buoyancy frequency exhibited a diurnal cycle above 40 m. The top two ADCP shear bins, centered at 29 and 41 m, showed a diurnal cycling. The cycling was strongest near the surface. The shallowest estimate of shear and N was at 17.5 m, calculated from the T44 current measurements at 10- and 25-m depth and the RSVP density estimates (Figure 7*a*). Temperatures measured by the RSVP and by sensors on the current meters were highly correlated (rms differences at 10 and 25 m were 0.18°C and 0.19°C, respectively). Some of the high-frequency noise may be due to separation of ship and buoy. Nevertheless, shear and N clearly cycle in phase with the same relative magnitude and with a diurnal periodicity. As a result, the Richardson number indicates almost no diurnal variability (Figure 7*b*). At depths below 40 m, the dominant period was more semidiurnal, but

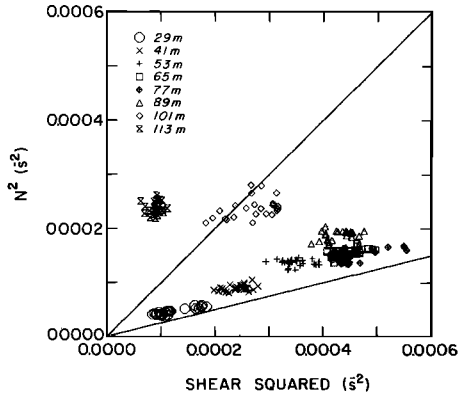

Fig. 8. Buoyancy frequency squared versus shear squared for eight different 12-m depth bins. An average daily cycle was created from the 12-day series. All hours of the day are plotted at each depth level. The first five depth bins follow the theoretical lower bound for critical Richardson number (slope of 0.25) quite closely. They lie in the shear maximum region. The three deeper bins were from the shear minimum region and reflect much higher Richardson numbers.

shear and N continued to track each other. We ended our station during a period of weak north-south current as the 20-day oscillation began a southward phase. Richardson numbers calculated for the days immediately following our station (using the mooring temperatures) indicated much larger Richardson number variability than we observed during our station. The large peak at the end of the Richardson number time series (Figure 7*b*) was the first of a period of high Richardson number variability with a diurnal periodicity.

The mutual tracking of shear and N that we observed during our station is apparent in ensemble averages. We formed an average daily cycle of shear and N using the 12 days of the time period. Each hour of the average day contains 12 independent estimates; thus at each depth there are 24 ensemble averaged estimates of shear and N. A plot of shear versus N at eight different depths indicates how strongly the two quantities track each other above the core (Figure 8). There was very little scatter in the averages at a given depth. The first five depth bins follow very closely (although they lie just above) the critical value of 0.25. These bins lie in the high-shear zone. At deeper bins, below the shear minimum region, the values of Richardson number were considerably higher. The low values of Richardson number above the core indicated that the dynamics of stratified shear flow instability were working to maintain a marginally stable flow field. Oceanic observations of Richardson numbers as low as 0.3 are rare; numbers less than 1 are usually considered critical. We note that Richardson numbers are very sensitive to the scales over which they are calculated and to the types of averaging that are applied.

The Richardson number results indicated a current system that could be easily destabilized to provide energy for turbulent mixing. The turbulent dissipations indicated that nighttime convection may be important in destabilizing the system, although the actual mechanism by which the turbulence is generated may be quite complicated. The mechanisms of how the convective mixing regime influences the deeper turbulence is the subject of a future investigation.

6. Conclusions

The Equatorial Undercurrent core, defined as the depth of the velocity maximum or alternatively the shear minimum, was very highly correlated with both the salinity maximum and with a σ_t surface. The core was most highly correlated with density, and it appeared to flow along a density surface. This result agreed with previous equatorial measurements indicating that the Equatorial Undercurrent lies within the thermocline; we believe that we were able to track these surfaces with 10-m accuracy and found that the correlation was indeed very high, even on time scales of 1 hour.

Velocity and displacement spectra were dominated by a peak at the semidiurnal internal tide; a change in slope was observed above and below this peak. With f scaling removed, equatorial spectral energies were comparable to those at midlatitude. Horizontal velocity spectra were found to be contaminated by the vertical displacement of the background shear.

Values of turbulent kinetic energy dissipation rate exhibited a diurnal cycle, with high values occurring at night. Shear and buoyancy frequency, calculated on 12-m vertical scales, tracked each other closely, dominated by a diurnal period above 40 m and semidiurnal below. The close tracking resulted in Richardson numbers that were marginally supercritical (between 0.3 and 0.6) in the high-shear region above the core, with no dominant periodicity. One interesting conclusion from the Richardson number statistics is that the theoretical lower bound of 0.25 appeared to be the lower bound in these measurements.

Acknowledgments. We thank M. Levine for many useful suggestions and discussions. We thank M. Park and R. Baumann for their help in the data analysis and the captain and crew of the R/V *Wecoma* for their cooperation during the field measurements. We also thank Dave Reinert for his expert preparation of the color diagrams. This work was supported by the National Science Foundation under contract OCE-8214639 as part of the Tropic Heat Program.

References

Caldwell, D. R., T. M. Dillon, and J. N. Moum, The rapid sampling vertical profiler–An evaluation, *J. Atmos. Oceanogr. Technol.*, *2*, 615–625, 1985.

Crawford, W. R., and T. R. Osborn, Control of equatorial currents by turbulent dissipation, *Science*, *212*, 539–540, 1981.

Desaubies, Y. J. F., Analytical representation of internal wave spectra, *J. Phys. Oceanogr.*, *6*, 976–981, 1976.

Duing, W., and Z. Hallock, Equatorial waves in the upper central Atlantic, GATE-2, *Deep Ses Res., Part A*, *26*, suppl. 2, 161–178, 1980.

Eriksen, C. C., Evidence for a continuous spectrum of equatorial waves in the Indian Ocean, *J. Geophys. Res.*, *85*, 3285–3303, 1980.

Fofonoff, N. P., Spectral characteristics of internal waves in the ocean, *Deep Sea Res.*, *16*, 59–71, 1969.

Garrett, C. J. R., and W. Munk, Space-time scales of internal waves, *Geophys. Fluid Dyn.*, *2*, 255–264, 1972.

Garrett, C. J. R., and W. Munk, Space-time scales of internal waves: A progress report, *J. Geophys. Res.*, *80*, 291–297, 1975.

Gregg, M. C., H. Peters, J. C. Wesson, N. S. Oakey and T. S. Shay, Intensive measurements of turbulence and shear in the equatorial undercurrent, *Nature*, *318*, 140–144, 1985.

Hayes, S. P., Vertical fine structure observations in the eastern equatorial Pacific, *J. Geophys. Res*, *86*, 10,983–10,999, 1981.

Legeckis, R., Long waves in the equatorial Pacific Ocean: A view from a geostationary satellite, *Science*, *197*, 1179–1181, 1977.

Levine, M. D., C. A. Paulson, and J. H. Morison, Internal waves in the Arctic Ocean: Comparison with lower-latitude observations, *J. Phys. Oceanogr.*, *15*(6), 800–809, 1985.

McPhaden, M. J., Fine-structure variability observed in CTD measurements from the central equatorial Pacific, *J. Geophys. Res.*, *90*(C6), 11,726–11,740, 1985.

Miles, J. W., and L. N. Howard, Note on a heterogeneous shear flow, *J. Fluid Mech.*, *20*, 331–336, 1964.

Moum, J. N., and D. R. Caldwell, Local influences on shear-flow turbulence in the equatorial ocean, *Science*, *230*, 315–316, 1985.

Moum, J. N., T. R. Osborn, and W. R. Crawford, Pacific equatorial turbulence: Revisited, *J. Phys. Oceanogr.*, in press, 1986*a*.

Moum, J. N, D. R. Caldwell, C. A. Paulson, T. K., Chereskin, and L. A. Regier, Does ocean turbulence peak at the equator?, *J. Phys. Oceanogr.*, in press, 1986*b*.

Munk, W., Internal waves and small scale processes in, *Evolution of Physical Oceanography*, edited by B. A. Warren and C. Wunsch, pp. 264–290, MIT Press, Cambridge, Mass., 1981.

Park, M. M., J. N. Moum, D. R. Caldwell, P. J. Stabeno, J. L. Cantey, and S. D. Wilcox, Tropic Heat 1984 rapid sampling vertical profiler observations, *Ref. 85-21*, 395 pp., College of Oceanography, Oregon State University, 1985.

Philander, S. G. H., Instabilities of equatorial currents, 2, *J. Geophys. Res*, *83*, 3679–3682, 1978.

Regier, L., Mesoscale current fields observed with a shipboard profiling acoustic meter, *J. Phys. Oceanogr.*, *12*, 880–886, 1982.

Toole, J. M., and S. P. Hayes, Finescale velocity-density characteristics and Richardson number statistics of the eastern equatorial Pacific, *J. Phys. Oceanogr.*, *14*, 712–726, 1984.

Wunsch, C., and S. Webb, The climatology of deep ocean internal waves, *J. Phys. Oceanogr*, *9*, 235–243, 1979.

Wyrtki, K., and B. Kilonsky, Transequatorial water structure during the Hawaii to Tahiti Shuttle Experiment, *Rep. 82-5*, 65 pp., Hawaii Inst. of Geophys., Univ. of Hawaii, Honolulu, 1982.

D. R. Caldwell, T. K. Chereskin, J. N. Moum, C. A. Paulson, and P. J. Stabeno, College of Oceanography, Oregon State University, Corvallis, OR 97331.

D. Halpern, School of Oceanography, University of Washington, Seattle, WA 98195.

L. A. Regier, Scripps Institution of Oceanography, La Jolla, CA 92093.

(Received April 28, 1986;
accepted May 20, 1986.)

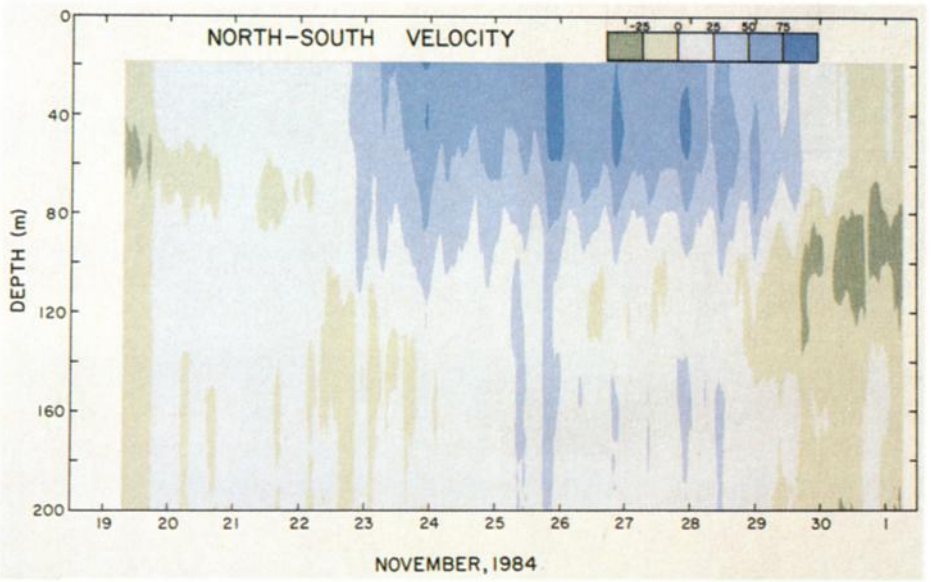

Plate 1*a*

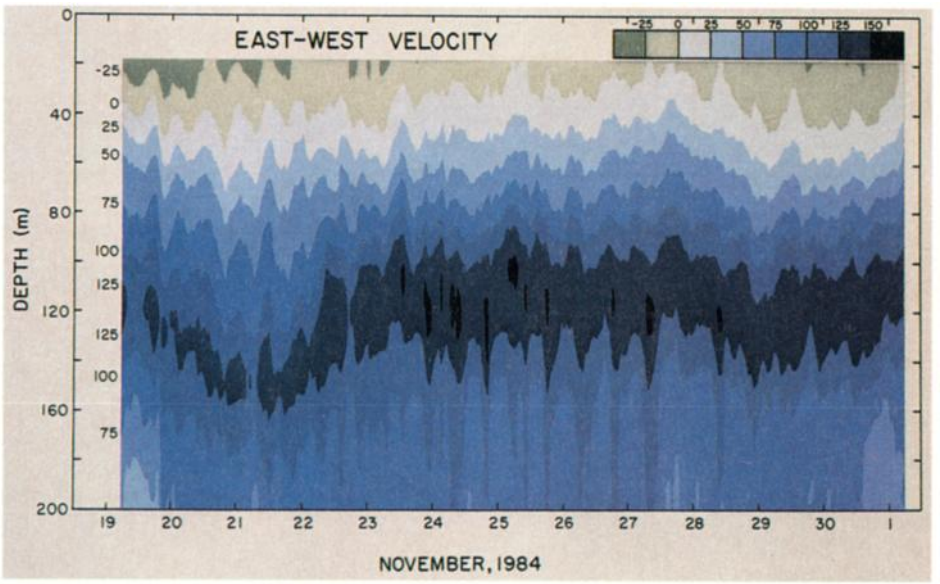

Plate 1*b*

Plate 1 [*Chereskin et al.*]. Hourly averages of (*a*) north-south current and (*b*) east-west current from the shipboard ADCP referenced using hourly currents at 25 m from the T44 buoy.

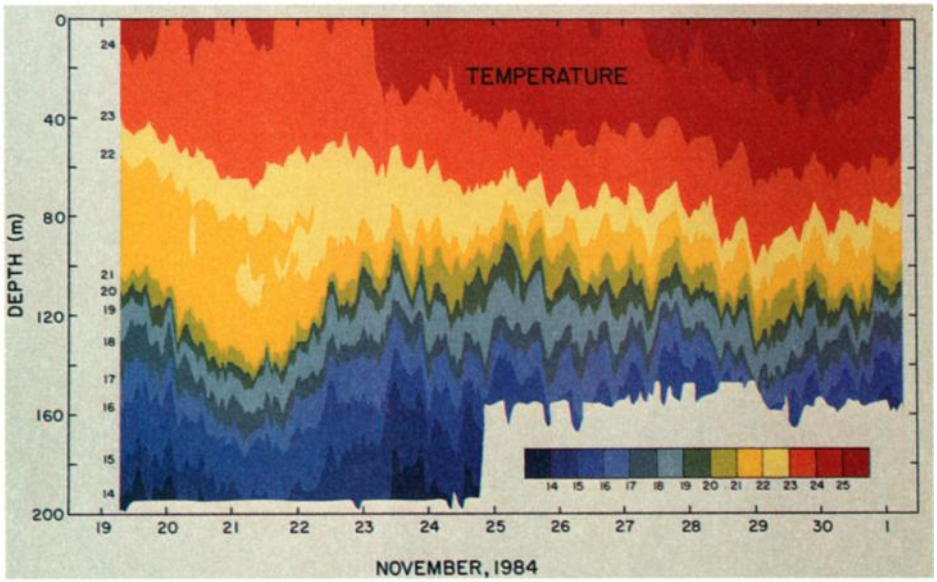

Plate 2*a*

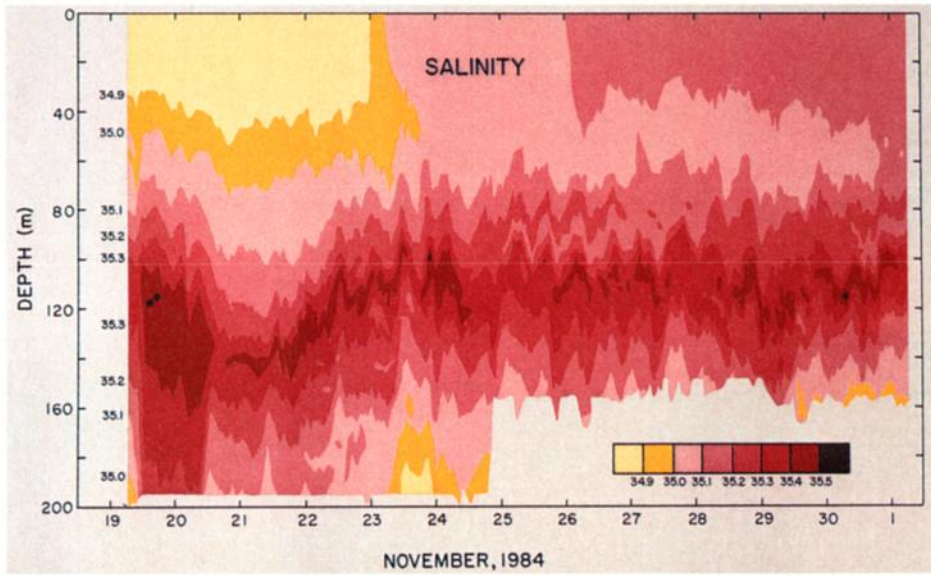

Plate 2*b*

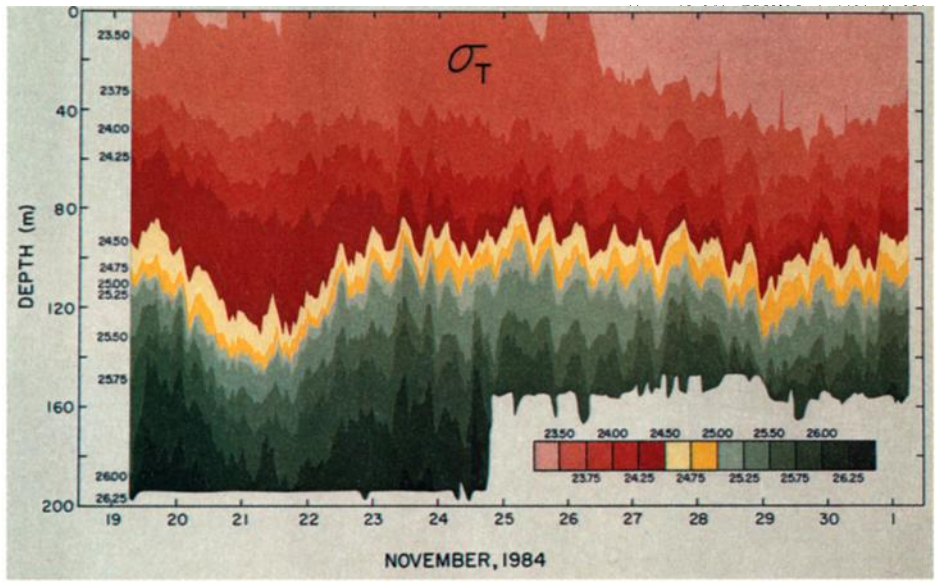

Plate 2*c*

Plate 2 [*Chereskin et al.*]. (*a*) Isotherm depths calculated from hourly averages of temperature in degrees Celsius. (*b*) Isohaline depths calculated from hourly averages of salinity in parts per thousand. (*c*) Isopycnal depths calculated from hourly averages of σ_t.

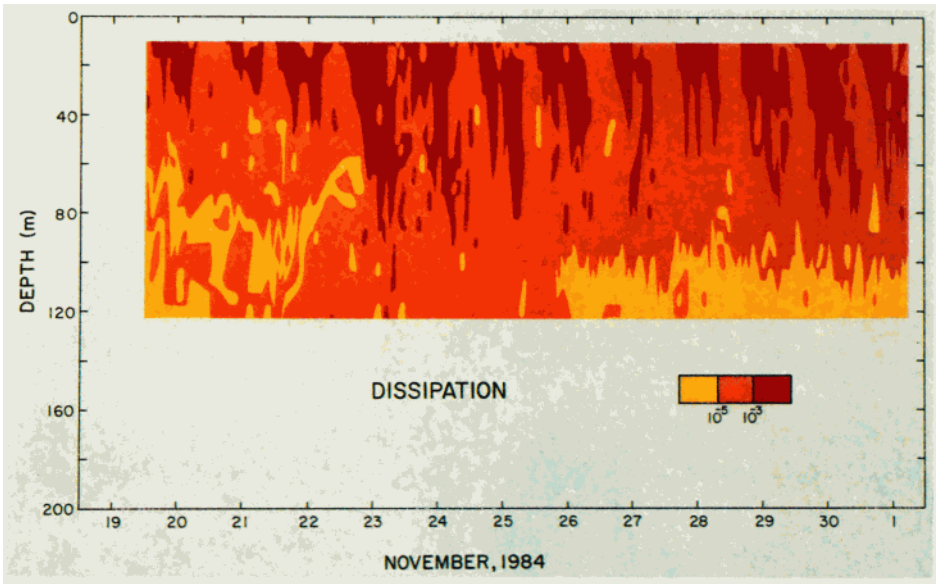

Plate 3 [*Chereskin et al.*]. Dissipation (in $cm^2\ s^{-3}$) contoured at 2-decade intervals, depth averaged over 5 m, and time averaged over 1 hour. High dissipations occur at night, with the deepest dissipations extending to 90 m.

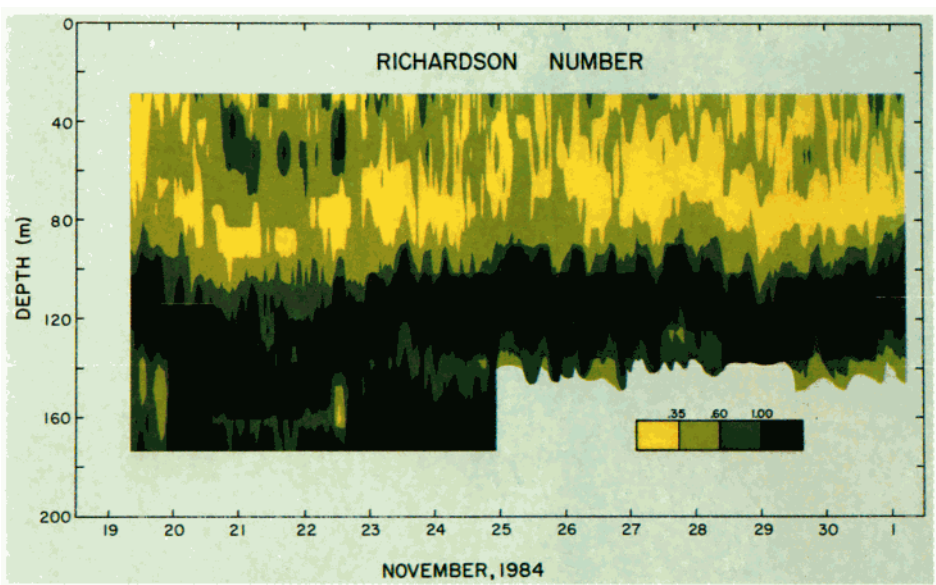

Plate 4 [*Chereskin et al.*]. Contours of hourly averaged Richardson number calculated over 12-m vertical scales (0.35, 0.60, and 1.00). Above the core the Richardson number was low (below 0.60). The core was distinguished as a region of high Richardson number (aobve 1.0). High values of Richardson number occurred above 75 m during the first 4 days, corresponding to lower shear associated with the pulse.